

Valley Polarization in Si(100) at Zero Magnetic Field

K. Takashina,¹ Y. Ono,¹ A. Fujiwara,¹ Y. Takahashi,^{1,*} and Y. Hirayama^{1,2}

¹NTT Basic Research Laboratories, NTT Corporation, Atsugi-shi, Kanagawa 243-0198, Japan

²SORST JST, Kawaguchi, Saitama 331-0012, Japan

(Dated: February 6, 2008)

The valley splitting, which lifts the degeneracy of the lowest two valley states in a SiO₂/Si(100)/SiO₂ quantum well is examined through transport measurements. We demonstrate that the valley splitting can be observed directly as a step in the conductance defining a boundary between valley-unpolarized and polarized regions. This persists to well above liquid helium temperature and shows no dependence on magnetic field, indicating that single-particle valley splitting and valley-polarization exist in (100) silicon even at zero magnetic field.

PACS numbers: 71.20.-b, 72.20.-i, 73.40.-c

Beyond its immense technological importance, silicon continues to command considerable physical interest. This, on one hand, is driven by relentless technological advances producing ever-higher-quality and versatile structures such as Silicon on Insulator (SOI) allowing unexplored physical regimes to be examined, and complementary processing techniques facilitating new experimental schemes[1]. On the other hand, silicon possesses a number of unique properties, a very fundamental one of which is its electronic band structure.

The conduction band dispersion relation of bulk silicon has 6 equivalent minima lying along three mutually orthogonal axes of the Brillouin Zone. With two-dimensional confinement parallel to one of these axes, this six-fold degeneracy is lifted such that the two minima lying along the confinement axis become the lowest lying states due to anisotropy of effective mass[2]. Electrons in 2-dimensional structures such as Si(100) MOSFETs (Metal Oxide Semiconductor Field Effect Transistors) occupy these remaining two valleys such that each electron has both valley and spin degrees of freedom. In recent years, this remaining valley degeneracy and valley splitting which lifts this degeneracy have experienced a revival of interest, partly because valleys offer a relatively unexplored degree of freedom in relation to metal-insulator transitions[3] and other many-body physics[4, 5, 6, 7, 8], but also due to new device possibilities[9, 10, 11] and as a source of decoherence in spin-based quantum computation[8, 10, 12].

Although effects indicating interactions between valleys have been known for a long time[13], they had been limited to structures involving vicinal planes which break the in-plane symmetry, or in (100) structures, special experimental conditions of low temperature and magnetic field[2]. Despite the long history, a consensus for the nature of this valley splitting has yet to be reached. In particular, some studies[6, 7, 8, 14] have pointed to a strong, almost linear, dependence on magnetic field, suggesting a many-body origin as opposed to a single-particle one, and its existence without magnetic field in Si(100) has not been experimentally confirmed.

In this Letter, we show the first direct and vivid evidence for valley splitting of Si(100) in the absence of magnetic field. Recent high magnetic field experiments have found that the Si/SiO₂ interface in SIMOX (Separation by IMplantation of OXygen (a type of SOI)) structures offer values of valley-splitting[15, 16] of at least a couple of meV, large compared with values found in conventional Si-MOS structures under equivalent conditions. Here, we show that the valley splitting in these structures can be increased to 10's of meV, and that this large valley splitting leads to a step feature in the conductance defining a boundary between valley-unpolarized and valley-polarized regions. This allows us to verify the existence of valley-splitting in the absence of magnetic field. Further, we find its effects to be important well above liquid helium temperatures and that the valley splitting can be approximated by a linear dependence on electrical bias even at unprecedentedly large values found here. These findings strongly suggest its single-particle nature, and demonstrate its potential for extensive band structure control and for examining new physical regimes where valley splitting is comparable to, or greater than, otherwise dominant energy scales.

The samples consist of SiO₂/Si(100)/SiO₂ quantum well transistors [Fig.1 (*inset*)] fabricated on SIMOX substrates where the buried oxide is formed through ion-implantation followed by high temperature annealing[16]. Data presented here come from a nominally 8nm wide quantum well clad between thermal and buried oxide layers 75nm and 380nm thick respectively, with large device dimensions of 30 μ m channel-width and 208 μ m between source and drain. The peak Hall mobility in these structures is 0.8m²/Vs. Front and back-gate capacitances were found to be $C_F = 485\mu\text{Fm}^{-2}$ and $C_B = 92\mu\text{Fm}^{-2}$ respectively agreeing with sample dimensions.

The source-drain current I_{SD} was measured as a function of front gate voltage V_{FG} at various values of back gate voltage V_{BG} [Fig.1] (at a constant source voltage (3mV) and constant temperature (4.2K), $G_{SD} = I_{SD}/3\text{mV}$). With V_{BG} set at zero volts, G_{SD} shows behavior characteristic of a standard silicon MOSFET at

low temperature. At first, carriers induced by V_{FG} are localized and do not contribute to conduction. With the electron number density n increased, they begin to conduct and G_{SD} shows a sharp increase. When negative V_{BG} is applied, the overall trace shifts to higher V_{FG} since the carrier concentration n also depends on V_{BG} according to $n = C_F(V_{FG} - V_F^{Th}) + C_B(V_{BG} - V_B^{Th})$ where V_F^{Th} and V_B^{Th} are constant offsets. Also, since the electric field increases, a shallower slope in $G_{SD}(V_{FG})$ results due to increased interface roughness scattering. Behavior at $V_{BG} \leq 0$ is virtually identical to conventional MOSFETs with substrate bias[2].

With positive V_{BG} , G_{SD} traces shift to lower V_{FG} and a minimum develops [A in Fig.1] due to the second subband, or alternatively worded, electron channels being present at both front and back interfaces [17]. These two layers couple to form bonding and antibonding states, hereon referred to as “spatial subbands”, and the extent to which these should be described as two “electric” subbands or two spatially separated layers depends on the potential bias of the quantum well and self-consistent effects[16, 17]. While interlayer coupling changes the wavefunction thereby affecting mobility [18, 19], the accessibility of the second subband allow further scattering processes[20, 21] which reduces the conductance. These inter-spatial-subband effects, which have already been examined in other systems[18], are expected to be involved in producing the minimum here.

Positive V_{BG} also shifts the wavefunction of the lower spatial subband closer to the buried-oxide interface with greater valley splitting[16]. With large positive values of V_{BG} , the data reveal another feature [B in Fig.1]. We interpret this also to be caused by intersubband effects, but rather than spatial subbands, we argue that this feature arises due to valley splitting leading to two valley subbands. At low V_{FG} , the conduction is solely due to the lower valley subband and the step feature represents

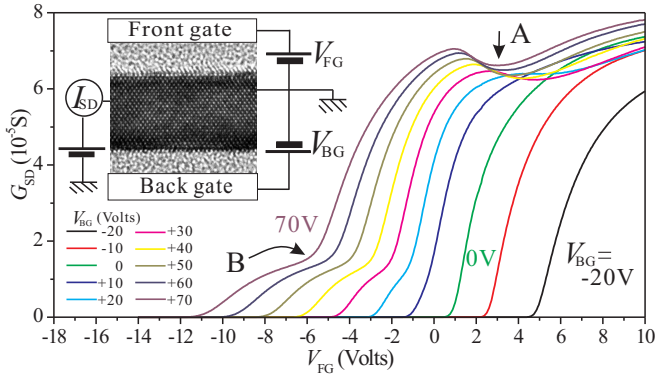


FIG. 1: (Color online) The source-drain conductance G_{SD} at 4.2K as a function of V_{FG} at different values of V_{BG} . A and B mark features due to second spatial subband and upper valley subband occupation respectively. The inset shows the experimental setup with a TEM image of a SIMOX structure.

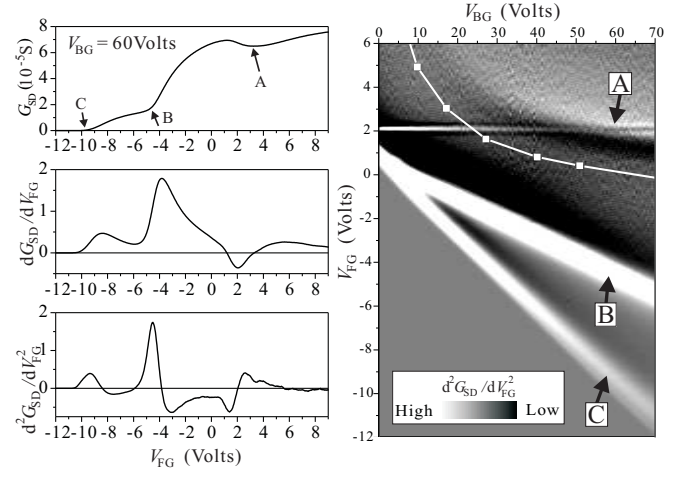


FIG. 2: *Left*: The conductance at $V_{BG} = 60V$, 4.2K. The lower two graphs show 1st and 2nd derivatives. The feature marked A is due to the second spatial subband. B marks the feature due to the upper valley while C marks the onset of conduction. *Right*: Gray-scale plot of the 2nd derivative showing the evolution of A, B and C with (V_{BG}, V_{FG}) . White squares show calculated onsets of second spatial-subband occupation [17]. The abrupt horizontal line at $V_{FG} = 2V$ is an experimental artifact.

the onset of occupation of the upper valley[22].

In order to examine the evolution of these features with V_{BG} , we doubly differentiate the $G_{SD}(V_{FG})$ traces to accentuate the features [Fig.2, left] and construct gray-scale plots as a function of (V_{BG}, V_{FG}) [Fig.2, right]. The initial onset of conduction and the subsequent step both appear as peaks in the double-differential, and as white regions on the gray-scale plot. While peak C at low V_{FG} marks the onset of conduction, peak B defines the boundary between valley polarized and unpolarized regions. It is readily seen that with increased V_{BG} , these peaks separate, and appear to continue separating in an approximately linear manner. The valley-polarized region grows in range as V_{BG} is increased indicating a linear increase in valley splitting Δ . This linear increase of Δ with V_{BG} and hence electric field is qualitatively consistent with theoretical predictions[2, 10] and previous magneto-transport estimates of the valley splitting[23].

To confirm that the structure arises due to valley-splitting, we performed measurements in magnetic field. Features similar to A, B and C at zero magnetic field can be seen at approximately the same (V_{BG}, V_{FG}) at $B = 5.5T$ (also marked A, B and C in Fig. 3(a)), demarcating regions showing different patterns of Shubnikov de Haas (SdH) oscillations. With positive V_{FG} and small V_{BG} (top-left of the graph) where the valley splitting Δ is known to be small, SdH oscillations can be seen with a period determined by the total filling factor $\nu^{tot} = nh/eB$. Minima are seen whenever ν^{tot} is an integer multiple of 4, since 4 is the combined degeneracy

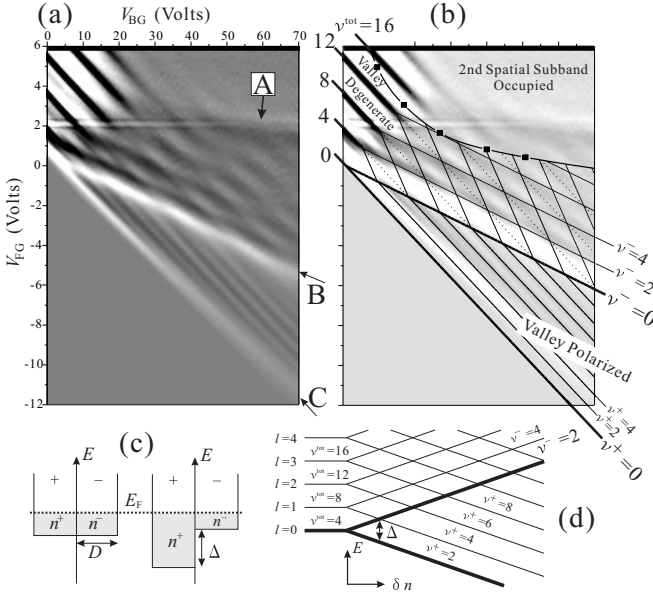


FIG. 3: (a) d^2G_{SD}/dV_{FG}^2 at 5.5T, 4.2K. (b) Same data as (a) but with different contrast. Solid squares joined by curves are estimated onsets of 2nd spatial subband occupation [17, 24]. Solid straight lines show calculated lines of even ν^+ and ν^- while dotted lines represent $\nu^{\text{tot}} = 4i$ where i is an integer [25]. The region beneath $\nu^- = 0$ is completely valley-polarized. (c) Density of states at zero magnetic field with and without valley splitting Δ . (d) Resultant Landau levels. Thicker lines also correspond to valley subband edges.

of valley and spin[2]. In contrast, in the region lying between features B and C, the oscillations occur with half the periodicity of $\Delta\nu^{\text{tot}} = 2$, showing that the only remaining degeneracy here is due to spin and the system is completely valley-polarized where the electrons only occupy the lower valley subband. In the region above B, two sets of oscillations can be seen. One set describes lines rather parallel to B, verifying that B represents the onset of the upper valley subband [24].

To make estimates of Δ , we use a simple phenomenological model. If each valley has identical and constant in-plane effective mass m^* , the density of states for each subband is $D = m^*m_0/\pi\hbar^2$. When both valleys have non-zero occupation, the number of electrons in each valley n^\pm is then given by $n^\pm = \frac{1}{2}(n \pm D\Delta)$ in which superscripts + and - indicate lower and upper valley states respectively [Fig.3(c)]. Since the directions along which the oscillations are occurring appear rather linear in (V_{FG}, V_{BG}) , we suppose a simple empirical approximation: $\Delta = \alpha\delta n$ when $\delta n > 0$ where $\delta n = n_B - n_F$, n_B and n_F being electron densities contributed by the back and front gates, respectively. (We set $\Delta = 0$ for $\delta n < 0$ since it is negligibly small.) It then follows that

$$n^\pm = \frac{1}{2}[(1 \mp D\alpha)n_F + (1 \pm D\alpha)n_B] \quad (1)$$

which can be used to calculate the filling factors of the

lower and upper valleys ν^+ and ν^- respectively under magnetic field [Fig.3(d)]. Solid lines in Fig.3 (b) show regions where ν^+ and ν^- are even, where the fitting parameter has been set to $\alpha = 0.46\text{meV}/10^{15}\text{m}^{-2}$ chosen to fit the minimum along $\nu^- = 2$. Although this value of α works reasonably well between $\nu^- = 0$ and $\nu^- = 4$, smaller values of around $\alpha = 0.40\text{meV}/10^{15}\text{m}^{-2}$ work better for higher filling factors between $\nu^- = 8$ and 10. This is likely to be due to the larger concentration leading to more screening, reducing the effect of the external bias. In turn, it also suggests that greater values are present at lower concentrations.

We have also performed measurements where the magnetic field was swept keeping V_{BG} constant at 60V which have shown that the SdH oscillations can be fitted to similar accuracy as the constant field data [Fig.3] without any magnetic field dependence of Δ . This confirms that the valley splitting here is independent of magnetic field, corroborating the correspondence between the data at zero field [Fig.2] and higher field [Fig.3].

Fig.4 shows G_{SD} and its second derivative taken at zero magnetic field and $V_{BG} = 60\text{V}$ where we estimate $\Delta = 23\text{meV}$ ($\Delta/k_B = 270\text{K}$) at the onset of upper valley occupation. The valley subband edges expected from the fit are also marked, suggesting that the actual bottom of the upper valley subband ($n^- = 0$) occurs at a lower value of V_{FG} than the center of the peak in d^2G_{SD}/dV_{FG}^2 . This is consistent with the interpretation that the step feature in G_{SD} arises as a consequence of suppression in mobility when the upper valley becomes energetically accessible. The step-like increase occurs when this suppression becomes weaker, after the onset of occupation, as the Fermi energy moves further above the subband edge. However, further work to establish the roles played by inter-valley interactions and the differences in mobility of the two individual valley subbands are required before a quantitative understanding of G_{SD} can be reached.

Fig. 4 also shows that the conduction band edge expected from the fit lies at lower V_{FG} than the onset of conduction. In Fig. 3, it is also seen, that although lines of constant ν^+ describe straight diagonal lines, the peak associated with the onset of conduction (C) curves

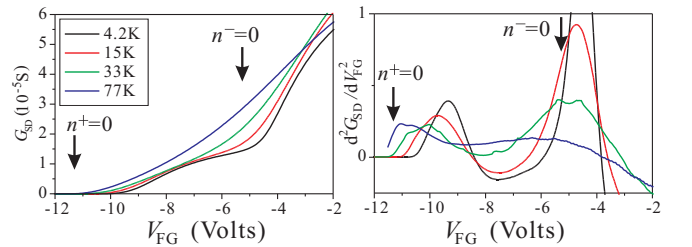


FIG. 4: (Color online) Temperature dependence at $B = 0\text{T}$, $V_{BG} = 60\text{V}$. Left: G_{SD} . Right: d^2G_{SD}/dV_{FG}^2 . Arrows mark valley subband edges extracted using $\alpha = 0.46\text{meV}/10^{15}\text{m}^{-2}$.

toward higher V_{FG} with increased V_{BG} . This can be attributed to increase in the number of localized states with V_{BG} as the disorder is increased, due in turn to the electrons being pressed against the Si-SiO₂ interface. With increased temperature, the peak in the second differential shifts toward the predicted conduction band edge.

At higher temperatures, the feature associated with the upper valley can still be discerned directly in G_{SD} at 33K, but it is not so clear at 77K. However, the double differential does show the second peak even at 77K. At such a temperature and above, the conduction globally becomes strongly influenced by phonon scattering and is no longer a good probe for detecting subband edges.

We now discuss our findings in relation to recent experiments in other systems. Studies on conventional Si MOS[6] and Si/SiGe[8] have both shown very strong dependence of Δ on magnetic field. In Si/SiGe, the absolute values of Δ are extremely small (10's of μ eV) suggesting that their phenomena belong to a completely different regime at very much smaller energy scales. In conventional Si MOS structures, Δ has relatively larger values between 0.2 and 2meV, but these are still smaller than values addressed in this work. Furthermore, the reported field dependence comes from measurements of energy gaps in the quantized Hall regime[6, 14] and their results are likely to be heavily influenced by many-body effects dominant under their conditions.

The results here suggest, therefore, that there exists a *bare* valley splitting arising from single particle interactions [10], independent of magnetic field. When it is of the order of a few meV and greater, it dwarfs many body contributions and there is very little magnetic field dependence. When the bare splitting is small, on the other hand, interaction effects become dominant and heavily influences the energy-gaps and its dependence on magnetic field.

There is also another important conclusion we can draw from the present results. In our previous experiments, we could only conclude that the valley splitting at the Si-buried oxide interface was much larger compared with the standard thermal-oxide interface at the front showing usual small values[16]. The linear dependence on electrical bias we find here, demonstrates that this rule is applicable even when the absolute value of Δ becomes orders of magnitude greater than those normally observed. What changes from one type of interface to another is the prefactor α .

This work is partially supported by JSPS KAKENHI (16206003) and (16206038).

9, Kita-ku, Sapporo, 060-0814 Japan

- [1] Examples of experiments using SOI include J. Gorman, D.G. Hasko and D.A. Williams, Phys. Rev. Lett., **95**, 090502 (2005), N. Pauc *et al.*, Phys. Rev. Lett., **92**, 236802 (2004), A. Fujiwara and Y. Takahashi, Nature, **410**, 560 (2001)
- [2] T. Ando, A.B. Fowler and F. Stern, Rev. Mod. Phys., **54**, 437 (1982)
- [3] A. Punnoose and A. M. Finkel'stein, Physica A, **302**, 318 (2001)
- [4] U. Zeitler *et al.*, Phys. Rev. Lett., **86**, 866 (2001), K. Lai *et al.*, Phys. Rev. Lett., **96**, 076805 (2006)
- [5] V.M. Pudalov *et al.*, cond-mat/0104347 (2001)
- [6] V.S. Khrapai, A.A. Shashkin and V.T. Dolgoplov, Phys. Rev. B, **67**, 113305 (2003)
- [7] Y.P. Shkolnikov *et al.*, Phys. Rev. Lett., **89**, 226805 (2002)
- [8] S. Goswami *et al.*, cond-mat/0408389 (2004)
- [9] Y. Hada and M. Eto, Phys. Rev. B, **68**, 155322 (2003), Y. Hada and M. Eto, JJAP, **43** 7329 (2004)
- [10] T.B. Boykin *et al.*, App. Phys. Lett., **84**, 115 (2004), T.B. Boykin *et al.*, Phys. Rev. B, **70**, 165325 (2004)
- [11] D. Ahn, S.W. Hwang and S-H. Park, quant-ph/0405037(2004)
- [12] B. Koiller, X. Hu, and S. Das Sarma, Phys. Rev. Lett., **88** 027903 (2002)
- [13] A.B. Fowler *et al.*, Phys. Rev. Lett., **16**, 901 (1966)
- [14] V.M. Pudalov, S.G. Semenchinsky, V.S. Edelman, JETP Letters, **41**, 325 (1985)
- [15] T. Ouisse *et al.*, Physica B, **249**, 731 (1998)
- [16] K. Takashina *et al.*, Phys. Rev. B, **69**, 161304(R), (2004)
- [17] We have performed self-consistent calculations neglecting valley-splitting and manybody effects to estimate (V_{FG} , V_{BG}) at the onset of 2nd subband occupation for an 8nm wide well. These are presented in Figs. 2 and 3(b) and agrees qualitatively with the behavior of feature A.
- [18] M. Prunnila, J. Ahopelto and H. Sakaki, Phys. Stat. Sol., **202**, 970 (2005)
- [19] A. Palevski *et al.*, Phys. Rev. Lett., **65**, 1929 (1990)
- [20] H.L. Störmer, A.C. Gossard, W. Wiegmann, Solid State Commun. **41**, 707 (1982)
- [21] X.G. Feng, D. Popovic and S. Washburn, Phys. Rev. Lett., **83**, 368 (1999)
- [22] Y.P. Shkolnikov *et al.*, App. Phys. Lett., **85**, 3766 (2004)
- [23] R.J. Nicholas, K. von Klitzing and Th.Englert, Solid State Commun., **34**, 51 (1980)
- [24] We observe no valley splitting feature like B for the upper spatial subband. This is because the wavefunction of the second spatial subband is never large close to the buried oxide interface in the accesible gate-voltage range.
- [25] We note that deepest SdH minima are seen when conditions $\nu^{\text{tot}} = 4i$ and $\nu^- = 2i$ are both met while those where $\nu^- = 2i$, $\nu^+ = 2i$ but $\nu^{\text{tot}} \neq 4i$ are not as pronounced. We speculate that this is due to many-body effects which occur at Landau level coincidences [26].
- [26] T. Jungwirth and A.H. MacDonald, Phys. Rev. B, **63**, 035305, (2000)

* Present Address: Graduate School of Information Science and Technology, Hokkaido University, Kita 14, Nishi